

Evolution of the Cluster Mass and Correlation Functions in a Λ CDM Cosmology

Joshua D. Younger¹, Neta A. Bahcall¹, and Paul Bode¹

ABSTRACT

The evolution of the cluster mass function and the cluster correlation function from $z = 0$ to $z \approx 3$ are determined using $\sim 10^6$ clusters obtained from high-resolution simulations of the current best-fit Λ CDM cosmology ($\Omega_m = 0.27$, $\sigma_8 = 0.84$, $h = 0.7$). The results provide predictions for comparisons with future observations of high redshift clusters. A comparison of the predicted mass function of low redshift clusters with observations from early Sloan Digital Sky Survey data, and the predicted abundance of massive distant clusters with observational results, favor a slightly larger amplitude of mass fluctuations ($\sigma_8 \sim 0.9$) and lower density parameter ($\Omega_m \sim 0.2$); these values are consistent within $1\text{-}\sigma$ with the current observational and model uncertainties. The cluster correlation function strength increases with redshift for a given mass limit; the clusters were more strongly correlated in the past, due to their increasing bias with redshift—the bias reaches $b \sim 100$ at $z=2$ for $M > 5 \times 10^{13} h^{-1} M_\odot$ clusters. The richness-dependent cluster correlation function, represented by the correlation scale versus cluster mean separation relation, $R_0 - d$, is generally consistent with observations. This relation can be approximated as $R_0 = 1.7 d^{0.6} h^{-1}$ Mpc for $d \sim 20 - 60 h^{-1}$ Mpc. The $R_0 - d$ relation exhibits surprisingly little evolution with redshift for $z < 2$; this can provide a new test of the current Λ CDM model when compared with future observations of high redshift clusters.

Subject headings: cosmology:observations-cosmology:theory-cosmological parameters-dark matter-galaxies:clusters:general-large-scale structure of the universe

1. Introduction

Clusters of galaxies, the most massive virialized structures in the universe, provide vital information about large-scale structure of the universe and place powerful constraints on

¹Princeton University Observatory, Princeton NJ 08544

cosmology (Bahcall 1988; Peebles 1993; Carlberg *et al.* 1997; Rosati, Borgani & Norman 2002; Henry 2004; and references therein). The abundance of clusters as a function of mass (i.e. the cluster mass function) and the evolution of this abundance with redshift are sensitive probes of both the present day density parameter (Ω_m) and the amplitude of mass fluctuations (σ_8); this provides a powerful test of the cosmological model (Peebles, Daly, & Juszkievicz 1989; Henry & Arnaud 1991; Bahcall & Cen 1992; Oukbir & Blanchard 1992; Barlett & Silk 1993; White *et al.* 1993; Viana & Liddle 1996; Eke, Cole, & Frenk 1996; Pen 1996; Cen 1998; Ikebe *et al.* 2002; Seljak 2002; Bahcall *et al.* 2003b; and references therein).

The spatial distribution of clusters of galaxies serves as a complementary test of the cosmological model; this cluster distribution is often described by the two-point cluster correlation function. The amplitude of the correlation function offers a strong test of the cosmology (Bardeen, Bond, & Efstathiou 1987; Bahcall & Cen 1992; Mann, Heavens & Peacock 1993; Holtzman & Primack 1993; Croft & Efstathiou 1994; Borgani *et al.* 1995). In fact, it was the unexpectedly strong observed cluster correlations (Bahcall & Soneira 1983) that provided the first evidence against the then standard $\Omega_m = 1$ SCDM models (Bahcall & Cen 1992; Croft *et al.* 1997; Borgani, Plionis, & Kolokotronis 1999; Governato *et al.* 1999; Colberg *et al.* 2000; and references therein). In addition, the evolution of the cluster correlation function with redshift, which has received comparatively less attention in the literature, is sensitive to the cosmology.

Taken together, the cluster mass and correlation functions provide two of the most powerful constraints on cosmological models. Predictions have become increasingly robust with larger and higher resolution cosmological simulations, made possible by recent growth in computing power combined with more sophisticated algorithms. Considerable progress has also been made on the observational front to determine cosmological parameters. Combining the recent WMAP data with finer-scale CMB experiments plus galaxy and Ly- α forest data, Spergel *et al.* (2003) determined a best-fit power law Λ CDM model. While further data will refine this model, the differences are likely to be small. As a further check of this model, we present in this work the simulated mass and correlation functions of clusters of galaxies, and their evolution with redshift, determined from mock sky survey cluster catalogs generated from a Λ CDM simulation of the current best-fit cosmological model (Spergel *et al.* 2003). We compare our results to the most recent observations, and lay the groundwork for comparison with future cluster observations at both low and high redshift. Such comparisons will provide important tests of the current cosmology, and will enable further improvements in the determination of cosmological parameters.

2. The Cluster Mass-Function and Its Evolution

For the simulation parameters we took those determined by Spergel *et al.* (2003) from the new WMAP data on the largest scales, supplemented by other CMB experiments, galaxy surveys, and Ly- α forest observations on smaller scales. Assuming a spatially flat power law Λ CDM universe, these are: matter density $\Omega_m = 0.27$, cosmological constant $\Lambda = 0.73$, power spectrum amplitude $\sigma_8 = 0.84$, spectral index $n_s = 0.96$, and $h = 0.7$ where $H_0 = 100h \text{ km-s}^{-1}\text{-Mpc}^{-1}$. The simulation used the TPM code (Bode & Ostriker 2003) to evolve $N = 1260^3 \approx 2 \times 10^9$ particles in a periodic box $1500h^{-1} \text{ Mpc}$ on a side. The particle mass is $m_p = 1.26 \times 10^{11} h^{-1} M_\odot$, and a cubic spline softening length of $17 h^{-1} \text{ kpc}$ was introduced. The simulation is discussed in more detail in Hopkins, Bahcall & Bode (2005).

Particle positions in a light cone covering one octant of the sky out to redshift $z = 3$ were saved to disk; snapshots of the entire simulation volume were also saved. Dark matter halos, which would house clusters of galaxies, were identified from the particle position data using a Friends-of-Friends (FOF) percolation algorithm, with a linking length of $b = 0.2$ times the mean particle separation (Lacey & Cole 1994). The cluster center was defined as the location of the most bound particle. Clusters identified using linking length parameters of $b = 0.16$ and 0.25 were examined for comparison, yielding similar results.

The mass function (MF) of clusters, $n(>M)$, represents the number density of clusters with mass greater than M . The constraints which the present day cluster MF places on the mean density parameter of the universe (Ω_m) and the amplitude of mass fluctuations (σ_8) are partially degenerate in $\Omega_m - \sigma_8$. Observations of the present day cluster MF have established that $\sigma_8 \Omega_m^{0.5} \approx 0.5$ (Henry & Arnaud 1991; Bahcall & Cen 1992; White, Efstathiou, & Frenk 1993; Eke, Cole, & Frenk 1996; Viana & Liddle 1996; Kitayama & Suto 1997; Pen 1998). This degeneracy can be broken by studying the evolution of the cluster MF with redshift (Peebles, Daly, & Juszkievicz 1989; Oukbir & Blanchard 1992, 1997; Eke, Cole, & Frenk 1996; Viana & Liddle 1996; Bahcall, Fan, & Cen 1997; Carlberg, Morris, Yee, & Ellingson 1997; Henry 1997, 2000; Bahcall & Fan 1998; Eke *et al.* 1998; Donahue & Voit 1999). Cluster evolution is exponentially dependent on σ_8^2 (Bahcall, Fan, & Cen 1997; Bahcall & Bode 2003), and as a result, the most massive clusters evolve strongly in a low- σ_8 , $\Omega_m = 1$ universe, producing a very low abundance of massive clusters at $z > 0.5$. Conversely, the evolution of rich clusters is significantly weaker in a $\sigma_8 \approx 1$ low- Ω_m universe, with a considerably higher cluster abundance at $z > 0.5$ as compared to lower- σ_8 models.

The simulated cluster MF was determined from the light cone outputs using cluster masses calculated according to typical masses used by observers, including: mass within fixed radii (relative to the center of the cluster) of $0.5 h^{-1} \text{ Mpc}$ comoving ($M_{0.5}$), $1.5 h^{-1} \text{ Mpc}$ comoving ($M_{1.5}$), $0.6 h^{-1} \text{ Mpc}$ physical ($M_{0.6}$), and also mass within a radius containing a

mean overdensity of 200 relative to the critical density (M_{200}). Minimum mass cutoffs were chosen in order to ensure the completeness of the cluster sample: $M_{0.5} > 1.6 \times 10^{13} h^{-1} M_{\odot}$; $M_{1.5} > 5 \times 10^{13} h^{-1} M_{\odot}$; $M_{0.6} > 3 \times 10^{13} h^{-1} M_{\odot}$; and $M_{vir} > 1.75 \times 10^{13} h^{-1} M_{\odot}$. The evolution of the cluster MF for $M_{0.5}$ is presented in Figure 1. These results can be used for comparison of predictions of the current cosmological model with future observations of high redshift clusters.

The cluster MF for $M_{0.6}$ and $z = 0.1 - 0.2$ was compared to the observed early Sloan Digital Sky Survey cluster MF for the same redshift and mass range (Bahcall *et al* 2003b; see also Bahcall *et al.* 2003a). The results are presented in Figure 2; also shown are the best analytic model fits. The observed data follow the same shape as the LCDM MF, but are systematically offset to slightly lower masses. This suggests that either a bias of $\sim 20\%$ (~ 1 -sigma) exists in the observed cluster mass calibration (the mass calibration is expected to improve for the larger upcoming sample of SDSS clusters) or that Ω_m is somewhat lower than used in the simulation. The best-fit parameters to the observed SDSS MF are $\Omega_m \approx 0.2$ and $\sigma_8 \approx 0.9$, as shown in Figure 2. These best-fit parameters are consistent with the current model parameters within the combined observational and model uncertainties.

The predicted abundance evolution of high mass clusters can be compared to observations at higher redshift. We use the mass threshold $M_{1.5} > 8 \times 10^{14} h^{-1} M_{\odot}$ and observed abundances of Bahcall & Bode (2003); the results are presented in Figure 3. At high redshift, the model predicts considerably fewer clusters than observed. This suggests that the amplitude of mass fluctuations σ_8 is larger than 0.84. Bahcall & Bode (2003) found a best fit value of $\sigma_8 = 0.9 \pm 0.1$ for these data. These results are consistent with the current cosmological parameter ($\sigma_8 = 0.84 \pm 0.04$) within the combined observational and model uncertainties. Both the local cluster MF and the evolution of massive clusters at high redshift thus suggest $\sigma_8 \approx 0.9$ and $\Omega_m \approx 0.2$. These results indicate a σ_8 value at the high end of the current best-fit model allowed range, with Ω_m at the lower end of the accepted range; both values are consistent within 1-sigma with the recent CMB and large-scale structure observations. Further observations are needed to narrow down the precise value of these cosmological parameters.

3. The Cluster Correlation Function and Its Evolution

The cluster correlation function (CF) is a statistical measure of how strongly clusters of galaxies cluster as a function of scale. The probability of finding a pair of clusters in volumes V_1 and V_2 , as a function of pair separation (r) is

$$dP = n^2(1 + \xi_{cc}(r))dV_1dV_2, \quad (1)$$

where n is the mean number density of clusters, and $\xi_{cc}(r)$ is the cluster CF. The spatial distribution of clusters of galaxies described by the cluster CF is sensitive to cosmological parameters (e.g. Bahcall & Cen 1992; Borgani, Plionis, & Kolokotronis 1999; Colberg *et al.* 2000; and references therein).

Observationally, the cluster CF is an order of magnitude stronger than that of individual galaxies: typical galaxy correlation scales are $\sim 5h^{-1}\text{Mpc}$, as compared to $\sim 20 - 25h^{-1}\text{Mpc}$ for the richest clusters (Bahcall & Soneira 1983; Klypin & Kopylov 1983; see also Bahcall 1988; Huchra *et al.* 1990; Postman, Huchra, & Guller 1992; Bahcall & West 1992; Peacock & West 1992; Dalton *et al.* 1994; Croft *et al.* 1997; Abadi, Lambas, & Muriel 1998; Lee & Park 1999; Borgani, Plionis, & Kolokotronis 1999; Collins *et al.* 2000; Gonzalez, Zaritsky, & Wechsler 2002; and references therein). Furthermore, the strength of the CF increases with cluster richness and mass (Bahcall & Soneira 1983). As a result, the rarest, most massive clusters exhibit the strongest correlations.

The richness dependence of the cluster CF has been confirmed observationally (see references above), and explained theoretically (Kaiser 1984; Bahcall & Cen 1992; Mo & White 1996; Governato *et al.* 1999; Colberg *et al.* 2000; Moscardini *et al.* 2000; Sheth, Mo, & Tormen 2001; and references therein). However, these analyses have been done at low redshift, $z < 0.5$. With observational data becoming available at higher redshifts, the expected evolution of the cluster correlation function is increasingly important as an independent test of the cosmological model. Analytic approximations to the evolution of cluster halo abundance, bias, and clustering have yielded some promising results (Mann, Heavens, & Peacock 1993; Mo & White 1996, 2002; Sheth, Mo, & Tormen 2001; Moscardini *et al.* 2001). However, numerical simulations can provide the most reliable comparison between theory and observations. We determine the expected cluster CF and its evolution for the current best-fit ΛCDM model using light-cone outputs from the N-body cosmological simulation discussed in §2. When compared with recent observational results at low redshift, this provides a test of the current cosmological model; at the same time the evolution of the ΛCDM CF provides detailed predictions for comparison with future observations of high redshift clusters.

The cluster CF was calculated as a function of separation using $\xi_{cc}(r) = F_{DD}(r)/F_{RR}(r) - 1$, where $F_{DD}(r)$ is the frequency of cluster pairs with comoving separation r , and $F_{RR}(r)$ is the frequency of pairs in a random catalog. The cluster CF was calculated for different mass thresholds for $M_{0.5}$ and M_{200} in several redshift bins: $z = 0-0.2$, $0.45-0.55$, $0.9-1.1$, $1.4-1.6$, and $1.9-2.2$. Because of the rapidly decreasing abundance of the most massive clusters with redshift, their CF is studied only at lower redshifts. Examples of the cluster CF at different redshifts are presented in Figure 4.

The cluster CF for each redshift bin and mass threshold was fit to a power law of the form $\xi_{cc}(r) = (r/R_0)^{-\gamma}$, where γ is the correlation slope and R_0 is the correlation scale. The fits were done over the linear range of the cluster CF ($r \leq 50h^{-1}\text{Mpc}$) for both a fixed slope of $\gamma = 2$, and for γ as a free fitting parameter. The results are similar for both methods, with the best fit free slope $\gamma \approx 1.8$ for $z < 1.5$. The slope is mildly richness-dependent, with more massive clusters showing a slightly steeper slope. The evolution of R_0 and γ with redshift is presented in Figure 5.

The correlation scale R_0 increases both with cluster mass and with redshift (see Figure 5). The steepening slope at high redshifts causes $R_0(z)$ to be slightly lower for a free γ as compared to that of a fixed $\gamma = 2$, but the evolutionary trend remains the same. The evolutionary increase of the cluster correlation scale with redshift is stronger for more massive clusters at higher redshift. For example, clusters with $M_{0.5} > 1.6 \times 10^{13}h^{-1}M_\odot$ have $R_0 \approx 10h^{-1}\text{Mpc}$ at $z = 0.15$, $R_0 \approx 13h^{-1}\text{Mpc}$ at $z = 1$, and $R_0 \approx 17h^{-1}\text{Mpc}$ at $z = 2$; while clusters with $M_{0.5} > 3.0 \times 10^{13}h^{-1}M_\odot$ have $R_0 \approx 12h^{-1}\text{Mpc}$ at $z = 0.15$, $R_0 \approx 17h^{-1}\text{Mpc}$ at $z = 1$, and $R_0 \approx 29h^{-1}\text{Mpc}$ at $z = 2$. The free slope fits yield similar results.

The cluster CF (using M_{FOF}) and the CF of the dark matter particles were also determined for simulation box snapshots at various redshifts, and fit to a power law with a fixed slope $\gamma = 2$. The correlation scale of clusters (R_0^{cl}), as before, increases with redshift. By contrast, the correlation scale of the mass (R_0^m) decreases with redshift, as expected. This is due to the fact that clusters of a given comoving mass represent higher density peaks of the mass distribution as the redshift increases, and thus exhibit enhanced clustering with increasing redshift (see also Cole & Kaiser 1989; Mo & White 1996, 2002; Sheth, Mo, & Tormen 2001; Moscardini *et al.* 2001). Figure 6 shows the evolution of the ratio R_0^{cl}/R_0^m with redshift, which follows the evolution of bias from $z = 0$ to 2, where bias is defined as $b^2 = \xi_{cc}/\xi_{mm} \approx (R_0^{cl}/R_0^m)^\gamma$. As seen in Figure 6, the ratio R_0^{cl}/R_0^m , and thus the bias b , increases from ~ 3 to ~ 100 (for $M_{FOF} > 5 \times 10^{13}h^{-1}M_\odot$ clusters) as the redshift increases from $z = 0$ to 2. Other mass clusters show a similar trend.

Another useful approach to studying the evolution of the cluster correlation function is the $R_0 - d$ relation, where R_0 is the fitted correlation scale and d is the mean intercluster comoving separation. For a larger mass limit objects are less abundant, and thus their mean separation d increases. These objects are also more biased, so an increasing R_0 with d is observed (Bahcall & Soneira 1983; Szalay & Schramm 1985; Bahcall 1988; Croft *et al.* 1997; Governato *et al.* 1999; Bahcall *et al.* 2003c; Padilla *et al.* 2004; and references therein). Thus, the evolution of the $R_0 - d$ relation allows us to investigate the change in correlation strength with cluster mass and with redshift. We present the $R_0 - d$ relation (using $M_{0.5}$ mass thresholds and a fixed γ) for several redshift bins in Figure 7. The results for a free γ

are shown in Figure 8.

The resulting R_0-d relation shows a surprising behavior; there is essentially no evolution with redshifts for $z < 2$ (using $M_{0.5}$ thresholds). Mass thresholds measured within a fixed overdensity (M_{200} and M_{FOF}) show slightly more evolution, but still surprisingly little. This redshift invariant $R_0 - d$ relation provides a powerful test of the cosmology when compared with upcoming observations of high redshift clusters.

Why is the $R_0 - d$ relation invariant with redshift? The invariance appears to be partly due to the relative constancy of the cluster mass hierarchy with redshift. That is, the halos which are the most massive at an early time tend to remain part of the population of the most massive objects. Consider a given comoving volume of space. The majority, but not all, of the N most massive clusters at $z = 0$ are among the N most massive clusters at higher redshift. The clusters that are not in the top N at higher redshift are, in turn, clusters lower down on the mass scale. In such a case, if the sample of clusters at a given mean comoving separation d is not dramatically different at different redshifts, it will yield similar correlation strengths R_0 , assuming that the clusters have not moved significantly over that time period. To confirm this, we select clusters using $M_{0.5}$ from box snapshots at $z=0$, 0.94, 1.4, and 2.0. A cluster at high redshift is considered to be the ‘matched’ system if it is within $3 h^{-1}\text{Mpc}$ physical separation of its position at $z = 0$. Using a fixed comoving mean separation $d = (N/V)^{-1/3}$ at all redshifts, the N_m clusters that match with their $z = 0$ counterpart are kept, and the remaining $N - N_m$ clusters are selected randomly from the next N clusters down the mass ladder. Using this new distribution, we find that the correlation scale $R_0(d, z)$ is indeed nearly constant with z for a given d (for $d \lesssim 90h^{-1}\text{Mpc}$ and $z < 2$). When looking along the past light cone, the $R_0 - d$ relation is thus nearly independent of redshift for $z < 2$ because the majority of clusters at different redshifts represent a similar population along the same filamentary hierarchical structure, near the top of the cluster mass hierarchy.

We compare the predictions of the ΛCDM model with current $R_0 - d$ observations in Figure 9, using $M_{0.5}$ thresholds and a fixed correlation slope of $\gamma = 2$ (for details on the observations see Table 1 of Bahcall *et al.* 2003c). All the observed correlation scales (R_0) and mean separations (d) were converted to comoving scales in a ΛCDM cosmology. The band in Figure 9 represents the simulated $R_0 - d$ relation (with $1-\sigma$ range) at $z = 0 - 0.3$ (to match the redshift range of the observations). An analytic approximation to the ΛCDM $R_0 - d$ relation for $20 \leq d \leq 60h^{-1}\text{Mpc}$, presented by the dashed curve, is

$$R_0 = 1.7 \left(\frac{d}{h^{-1}\text{Mpc}} \right)^{0.6} h^{-1} \text{Mpc} \quad . \quad (2)$$

The results show a general agreement between the ΛCDM model and observations. The op-

tically selected cluster samples agree with the model within $1\text{-}\sigma$. There is, however, a wide scatter at the high- d end, especially when X-ray selected clusters are included; the X-ray selected clusters seem to suggest a somewhat larger R_0 than optically selected clusters. Due to this large scatter, the correlation function cannot yet provide a high-precision determination of cosmological parameters. It does, however, clearly rule out high- Ω_m models, as their far weaker correlations are inconsistent with the data. The strong correlations suggested by the current X-ray clusters will be tested with future observations of X-ray selected cluster samples; this should clarify whether or not the X-ray clusters are consistent with the optical data and with the best-fit Λ CDM cosmology.

4. Conclusions

We use light cone outputs from a large-scale simulation of the currently best-fit Λ CDM cosmological model to generate mock sky survey cluster catalogs that can be readily compared with observations. The catalogs were used to determine the present day cluster mass and correlation functions, which together constitute a sensitive test of the cosmological model. We determine the evolution of the cluster mass function from $z = 0$ to $z = 3$, and the evolution of the cluster correlation function from $z = 0$ to $z = 2$. These results provide predictions of the current cosmological model for comparison with future observations of high redshift clusters. Such comparisons can be used to test the current model and provide new and independent constraints on both the cosmological density parameter, Ω_m , and the amplitude of mass fluctuations, σ_8 .

The simulated cluster mass function at low redshift ($z=0.1\text{--}0.2$) is compared with the early Sloan Digital Sky Survey cluster mass function (SDSS: Bahcall *et al.* 2003b). The Λ CDM mass function predicts somewhat higher abundances than are observed. This suggests that either a small bias ($\sim 20\%$) exists in the observed cluster mass calibration, or a somewhat lower value of the cosmological density parameter is needed ($\Omega_m \approx 0.2$). The results, however, are consistent with the current cosmology within the combined observational uncertainties. The evolution of the most massive clusters is exponentially dependent on σ_8^2 (Bahcall & Fan 1998), and therefore can be used to break the $\Omega_m - \sigma_8$ degeneracy that exists in the low-redshift mass function. We find that the Λ CDM model predicts a considerably lower abundance of distant ($z > 0.5$) massive clusters than observed. This suggests a normalization of $\sigma_8 \approx 0.9$.

We determine the cluster correlation function in the Λ CDM cosmology as a function of cluster mass threshold, summarized in the $R_0 - d$ relation (Figure 7–8). We find good agreement with observations of optically selected clusters (Figure 9); X-ray selected clusters

appear to suggest somewhat increased cluster correlations. The wide scatter in the observational data at high- d , makes it difficult at this time to provide precise constraints on the cosmology. The data are, however, in good agreement with the current Λ CDM model.

We determine the evolution of the richness dependent cluster correlation function in the Λ CDM cosmology (Figures 4 – 8). For a given mass limit, the correlation strength increases with redshift. Surprisingly, the $R_0 - d$ relation shows no significant evolution out to $z < 2$. This surprising result provides a new, independent test of the current cosmological model when compared with future observations of high redshift clusters.

We thank J.P. Ostriker, D. Spergel, and M. Strauss for helpful discussions. The computations were performed on the National Science Foundation Terascale Computing System at the Pittsburgh Supercomputing Center. This work was supported in part by NSF grant AST-0407305.

REFERENCES

- Abadi, M., Lambas, D., & Muriel, H. 1998, ApJ, 507, 526
- Bahcall, N.A. & Soneira, R.M. 1983, ApJ, 270, 20
- Bahcall, N.A. 1988, ARA&A, 26, 631
- Bahcall, N.A. & Cen, R. 1992, ApJ, 398, L81
- Bahcall, N.A. & West, M.J. 1992, ApJ, 392, 419
- Bahcall, N.A., Fan, X., & Cen, R. 1997, ApJ, 485, L53
- Bahcall, N.A. & Fan, X. 1998, ApJ, 504, 1
- Bahcall, N.A. *et al.* 2003a, ApJS, 148, 243
- Bahcall, N.A. *et al.* 2003b, ApJ, 585, 182
- Bahcall, N.A., Dong, F., Hao, L., Bode, P., Annis, J., Gunn, J.E., & Schneider, D.P. 2003c, ApJ, 599, 814
- Bahcall, N.A., & Bode, P. 2003, ApJ, 588, 1
- Bardeen, J. M., Bond, J. R., & Efstathiou, G. 1987, ApJ, 321, 28

- Barlett, J. G. & Silk, J. 1993, ApJ, 407, L45
- Bode, P. & Ostriker, J.P. 2003, ApJS, 145, 1
- Borgani, S., Plionis, M., Coles, P., & Moscardini, L. 1995, MNRAS, 277, 1191
- Borgani, S., Plionis, M., & Kolokotronis, V. 1999, MNRAS, 305, 866
- Carlberg, R.G., Morris, S.L., Yee, H.K.C., & Ellingson, E. 1997, ApJL, 479, L19
- Cen, R. 1998, ApJ, 509, 494
- Colberg, J.M. *et al.* 2000, MNRAS, 319, 209
- Cole, S. & Kaiser, N. 1989, MNRAS, 237, 1127
- Collins, C. *et al.* 2000, MNRAS, 319, 939
- Croft, R. A. C. & Efstathiou, G. 1994, MNRAS, 267, 390
- Croft, R.A.C. *et al.* 1997, MNRAS, 291, 305
- Dalton, G.B. *et al.* 1994, MNRAS, 271, L47
- Donahue, M. & Voit, G.M. 1999, ApJ, 523, L137
- Eke, V.R., Cole, S., & Frenk, C.S. 1996 MNRAS, 282, 263
- Eke, V.R., Cole, S., Frenk, C.S., & Henry, P.J. 1998, MNRAS, 298, 1145
- Gonzalez, A.H., Zaritsky, D., Wechsler, R.H. 2002, ApJ, 571, 129
- Governato, F. *et al.* 1999, MNRAS, 307, 949
- Henry, J.P. & Arnaud, K.A. 1991, ApJ, 372, 410
- Henry, J.P. 1997, ApJ, 489, L1
- Henry, J.P. 2000, ApJ, 534, 565
- Henry, J.P., 2004 ApJ, 609, 603
- Holtzman, J. A. & Primack, J. R., 1993, ApJ, 405, 428
- Hopkins, P.F., Bahcall, N.A., & Bode, P. 2005, ApJ, 618, in press
- Huchra, J., Henry, J.P., Postman, M., & Geller, M. 1990, ApJ, 365, 66

- Ikebe, Y., Reiprich, T.H., Bohringer, H., Tanaka, Y. & Kitayama, T. 2002, A&A, 383, 773
- Kaiser, N. 1984, ApJ, 284, L9
- Kitayama, T. & Suto, Y. 1997, ApJ, 490, 557
- Klypin, A. & Kopylov, A.I. 1983, Soviet Astron. Lett. 9,41
- Lacey, C. & Cole, S. 1994, MNRAS, 271, 676
- Lee, S. & Park, C. 1999 JKAS, 32, 1
- Mann, R.G., Heavens, A.F., & Peacock, J.A. 1993, MNRAS, 263, 798
- Mo, H.J & White, S.D.M. 1996, MNRAS, 282, 347
- Mo, H.J. & White, S.D.M. 2002, MNRAS, 336, 112
- Moscardini, L., Matarrese, S., Lucchin, F., & Rosati, P. 2000, MNRAS, 316, 283
- Moscardini, L., de Grandi, S., Lucchin, F., Matarrese, S., & Rosati, P. 2001 MmSAI, 72, 819
- Nichol, R.C., Collins, C.A., Guzzo, L., & Lumsden, S.L. 1992, MNRAS, 255P, 21
- Oukbir, J. & Blanchard, A. 1992, A&A, 262, L21
- Oukbir, J. & Blanchard, A. 1997, A&A, 317, 1
- Padilla, N.D., et al. 2004, MNRAS, 352, 211
- Peacock, J.A. & West, M.J. 1992, MNRAS, 327, 422
- Peebles, P.J.E. 1993, Principles of Physical Cosmology, Princeton University Press: Princeton
- Peebles, P.J.E., Daly, R.A., & Juszkievicz, R. 1989, ApJ, 347, 563
- Pen, Ue-Li 1998, ApJ, 498, 60
- Postman, M., Huchra, J., & Geller, M. 1992, ApJ, 384, 404
- Rosati, P., Borgani, S. & Norman, C. 2002, ARA&A, 40, 539
- Seljak, U. 2002, MNRAS, 337, 769
- Sheth, R.K., Mo, H.J., & Tormen, G. 2001, MNRAS, 323

- Spiegel, D.N., Verde, L., Peiris, H.V. Komatsu, E., Nolte, M.R., Bennett, C.L., Halpern, M., Hinshaw, G., Jarosik, N., Kogut, A., Limon, M. Meyer, S.S., Page, L., Tucker, G.S., Welland, J.L., Wollack, E., & Wright, E.L. 2003, ApJS, 148, 175
- Szalay, A.S. & Schramm, D.N. 1985, Nature, 314, 718
- Viana, P.P. & Liddle, A.R. 1996, MNRAS, 281, 323
- White, S.D.M, Efstathiou, G., & Frenk, C.S. 1993, MNRAS, 262, 1023

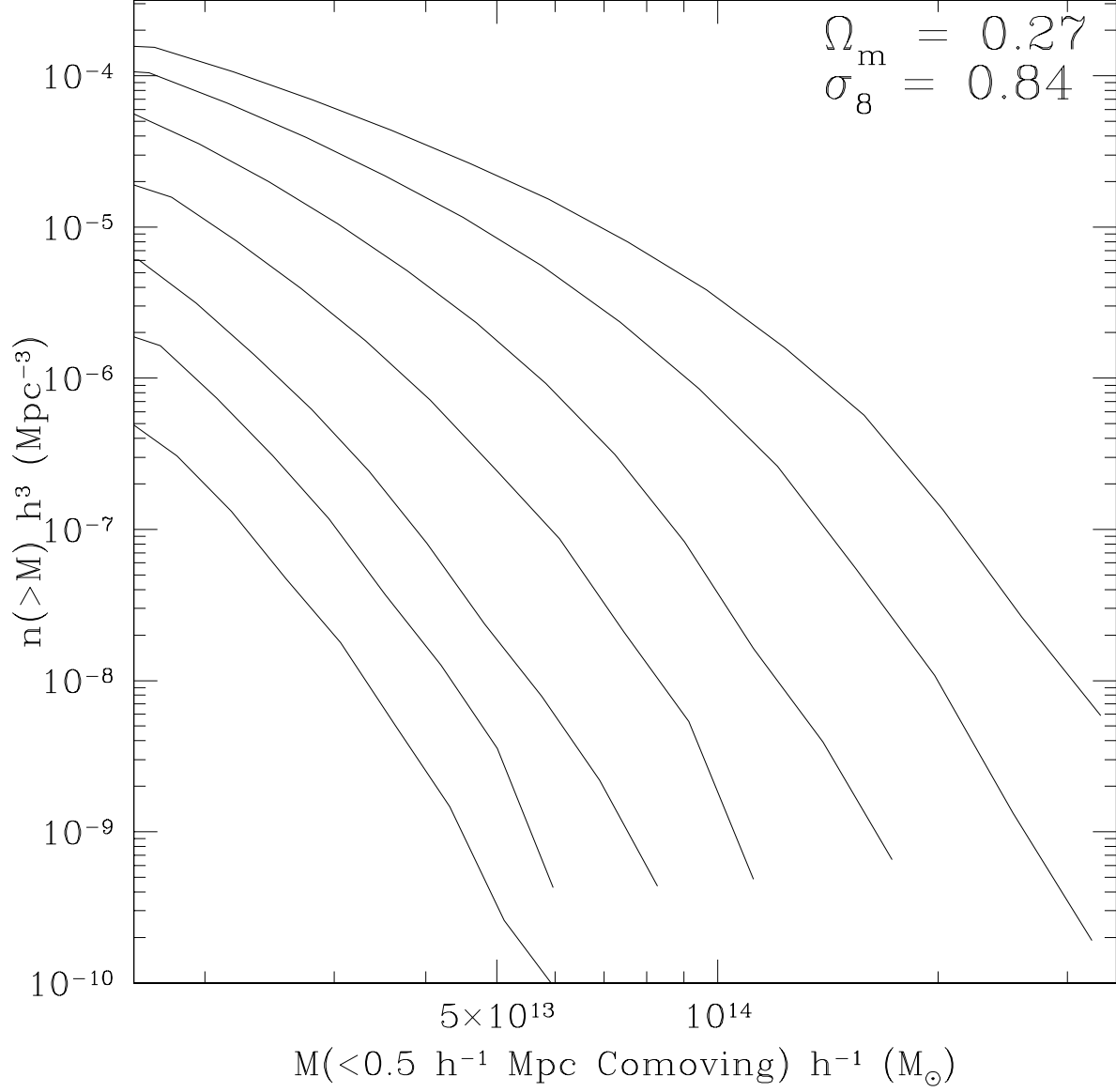


Fig. 1.— The simulated cluster mass function for Λ CDM, in redshift bins $z=0.0\text{--}0.15$; $0.45\text{--}0.55$; $0.95\text{--}1.05$; $1.45\text{--}1.55$; $1.9\text{--}2.1$; $2.2\text{--}2.5$; and $2.5\text{--}3.0$ (top to bottom). The mass $M_{0.5}$ is measured within a fixed comoving radius $0.5 h^{-1}\text{Mpc}$ from the cluster center.

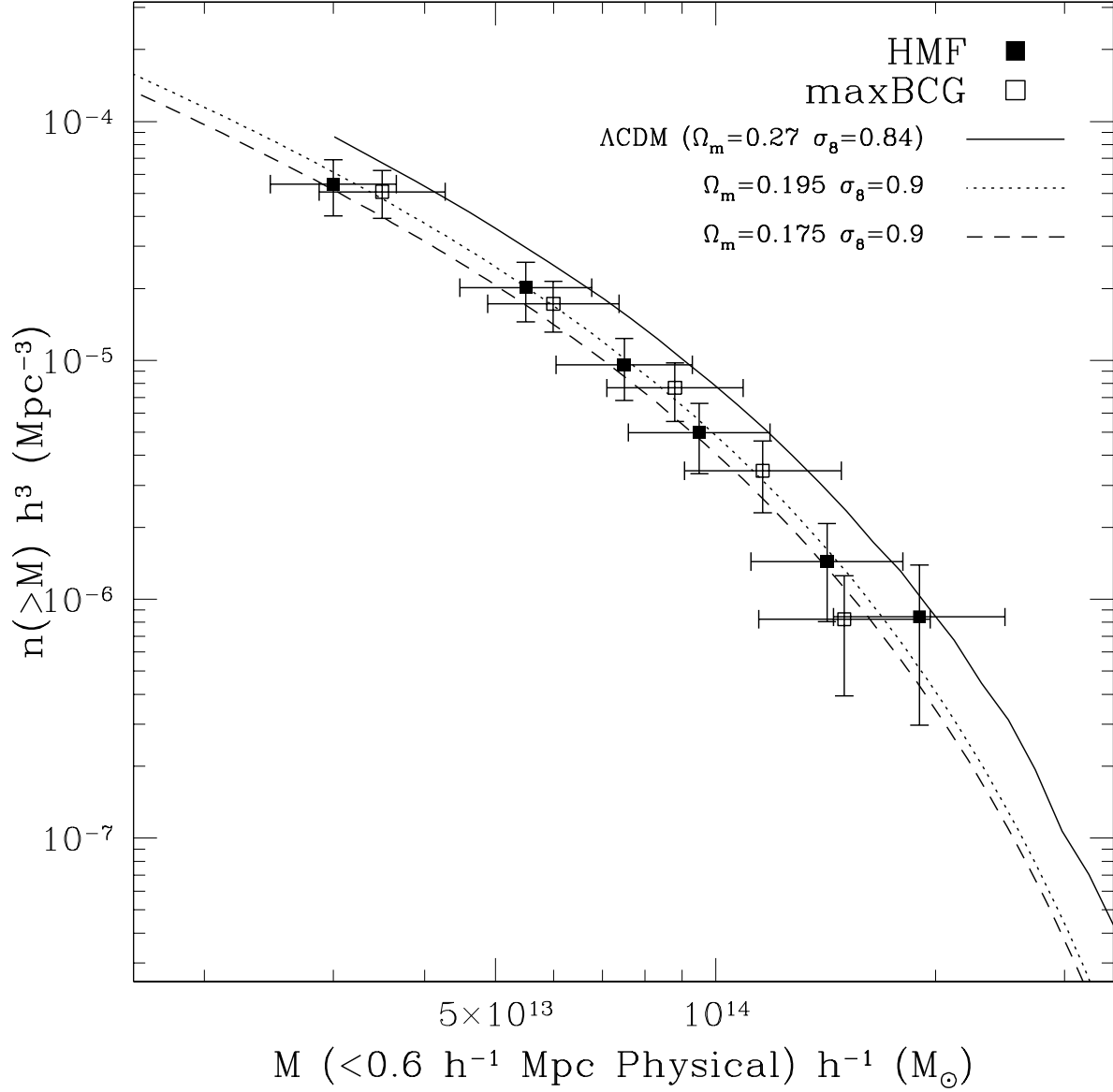


Fig. 2.— A comparison of the SDSS observed cluster MF and analytic best fits for the HMF (filled square, dashed line) and maxBCG (open square, dotted line) selection techniques (Bahcall *et al.* 2003a,b) and the current Λ CDM simulation predictions for $z = 0.1 - 0.2$. All masses are defined within a physical radius of $0.6 h^{-1}$ Mpc of the cluster center.

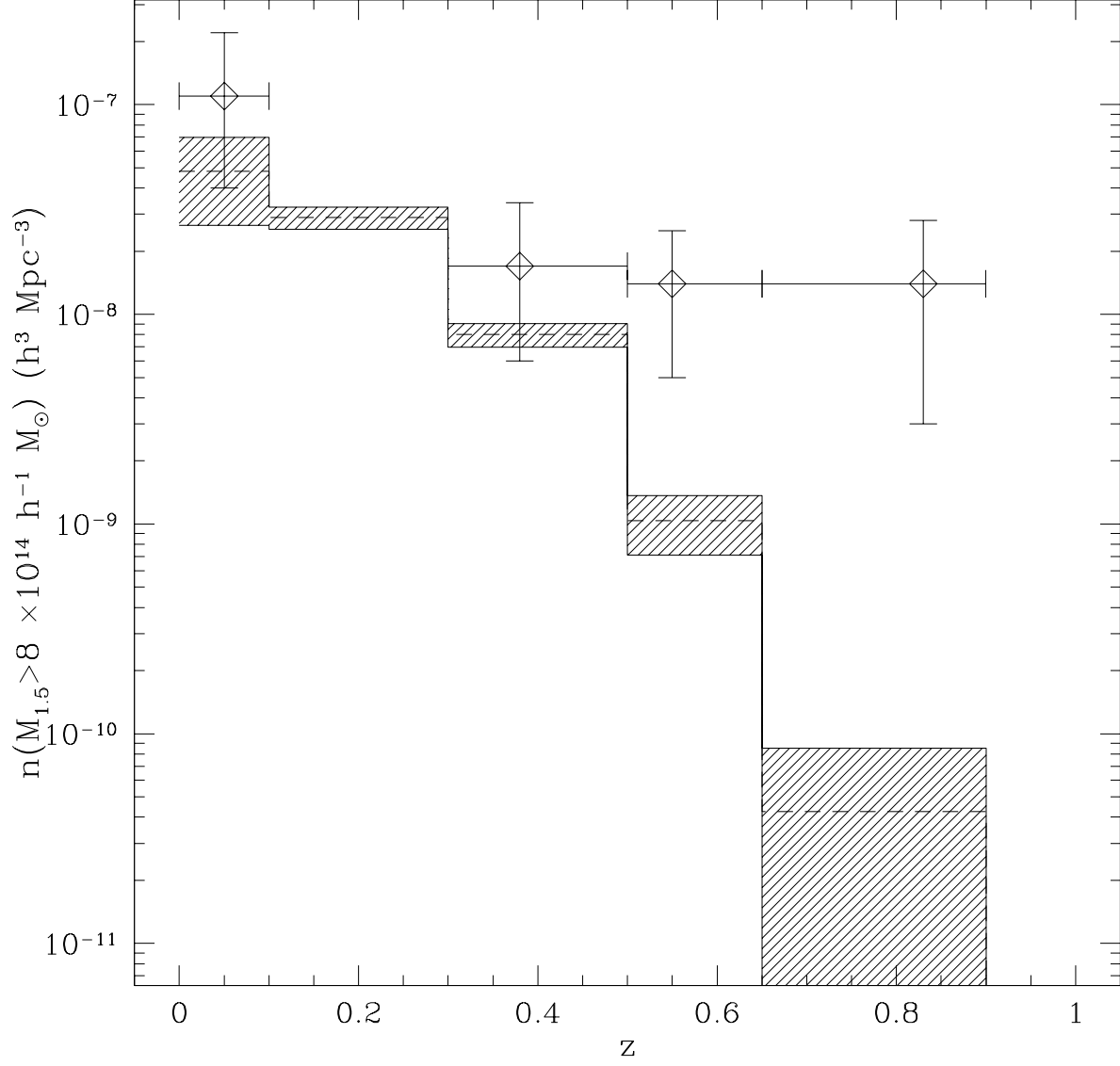


Fig. 3.— The cluster abundance evolution for massive clusters ($M_{1.5} > 8 \times 10^{14} h^{-1} M_{\odot}$) in the Λ CDM model (dashed line) versus observed abundances (1- σ Poisson error bars).

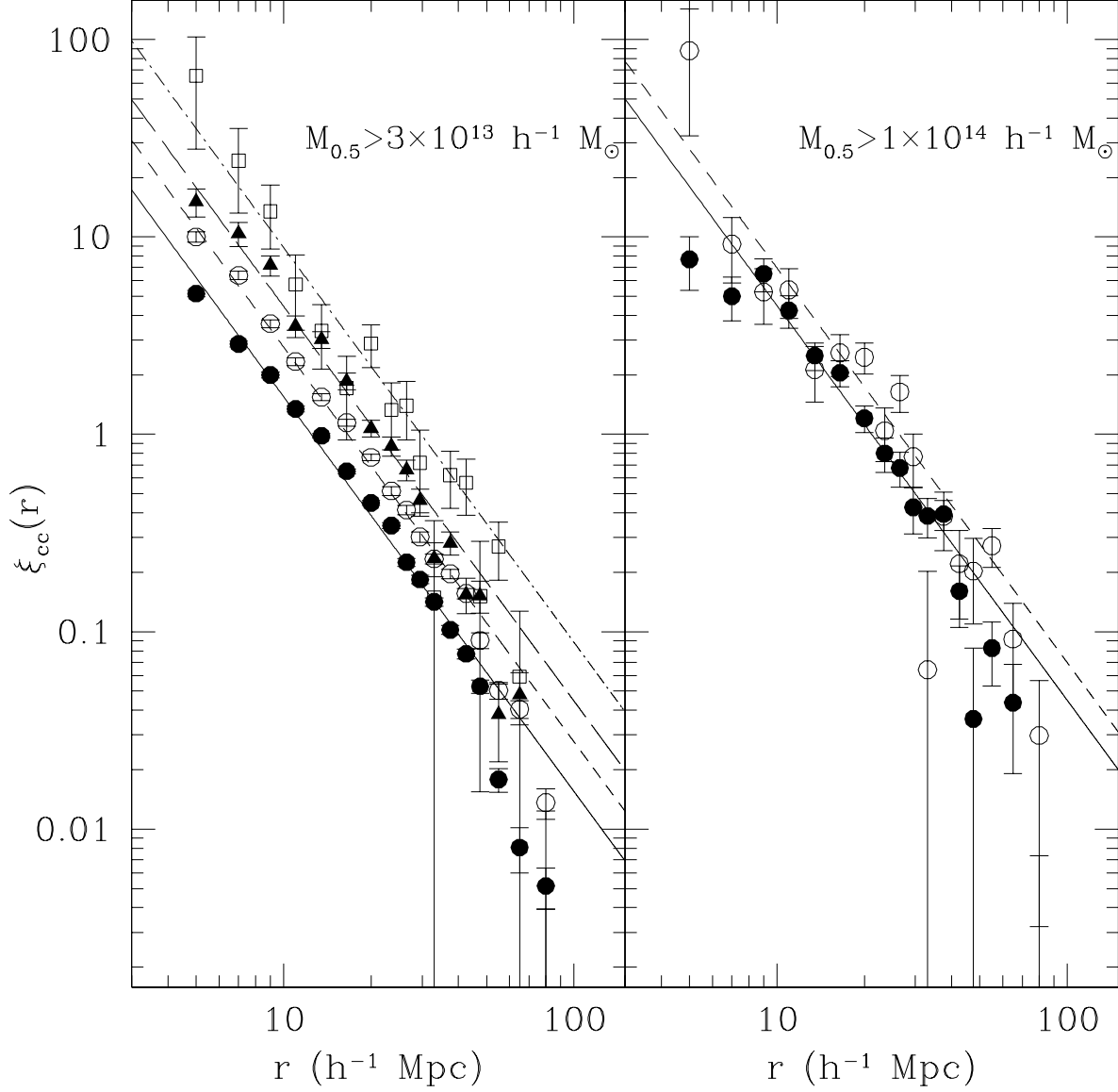


Fig. 4.— The simulated cluster correlation function for different redshift bins. From bottom to top: filled circles, $z=0.0-0.2$; open circles, $0.9-1.1$; filled triangles, $1.4-1.6$; open squares, $1.9-2.2$; with $1-\sigma$ Poisson error bars. The separation (r) is in comoving units, and the masses are measured within a fixed comoving radius of $0.5 h^{-1}$ Mpc. The lines represent the best fit power laws for a fixed correlation slope $\gamma = 2$.

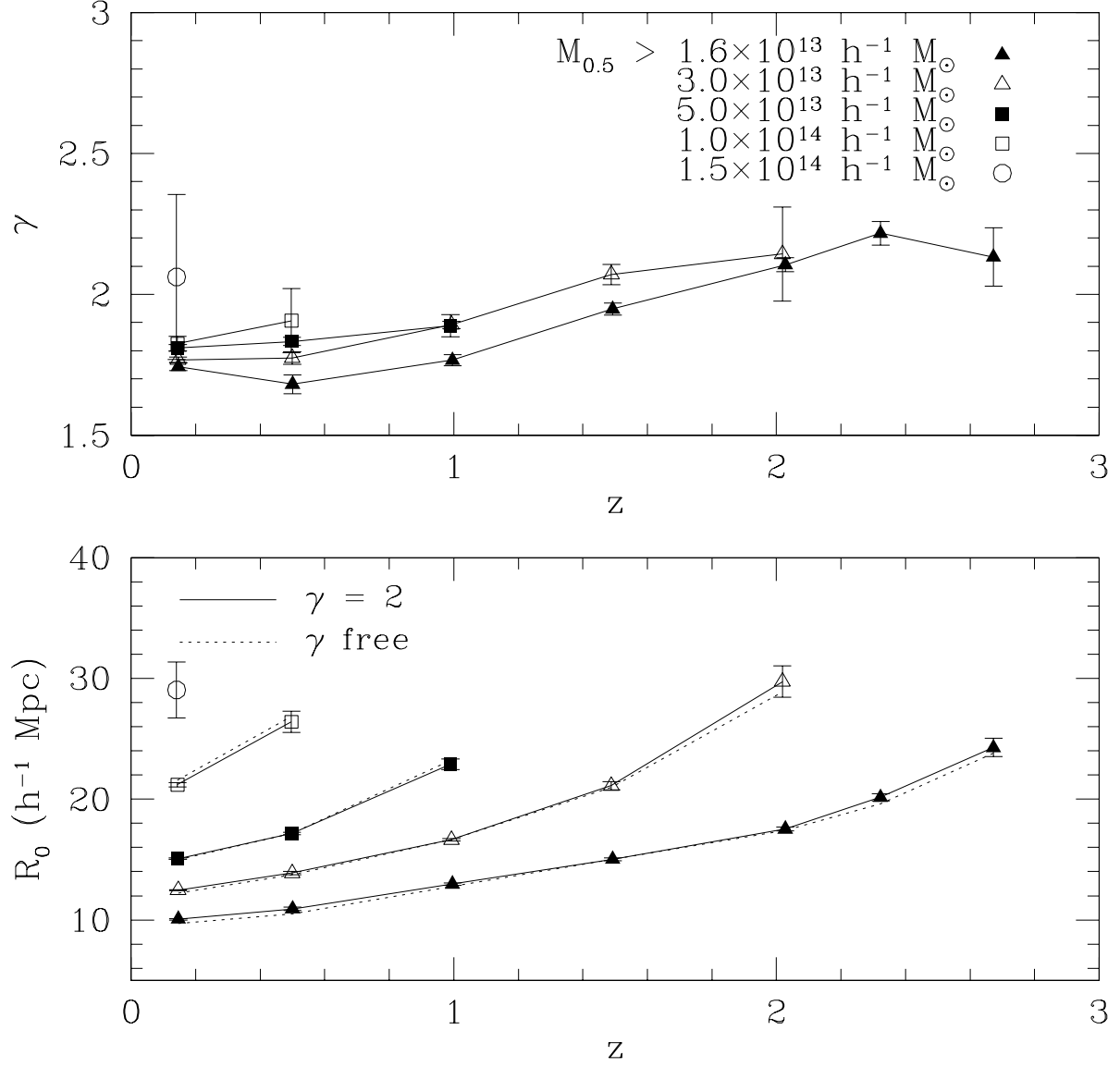


Fig. 5.— Evolution of the cluster correlation scale (R_0 comoving) and slope (γ) as a function of redshift for different mass thresholds for the Λ CDM model.

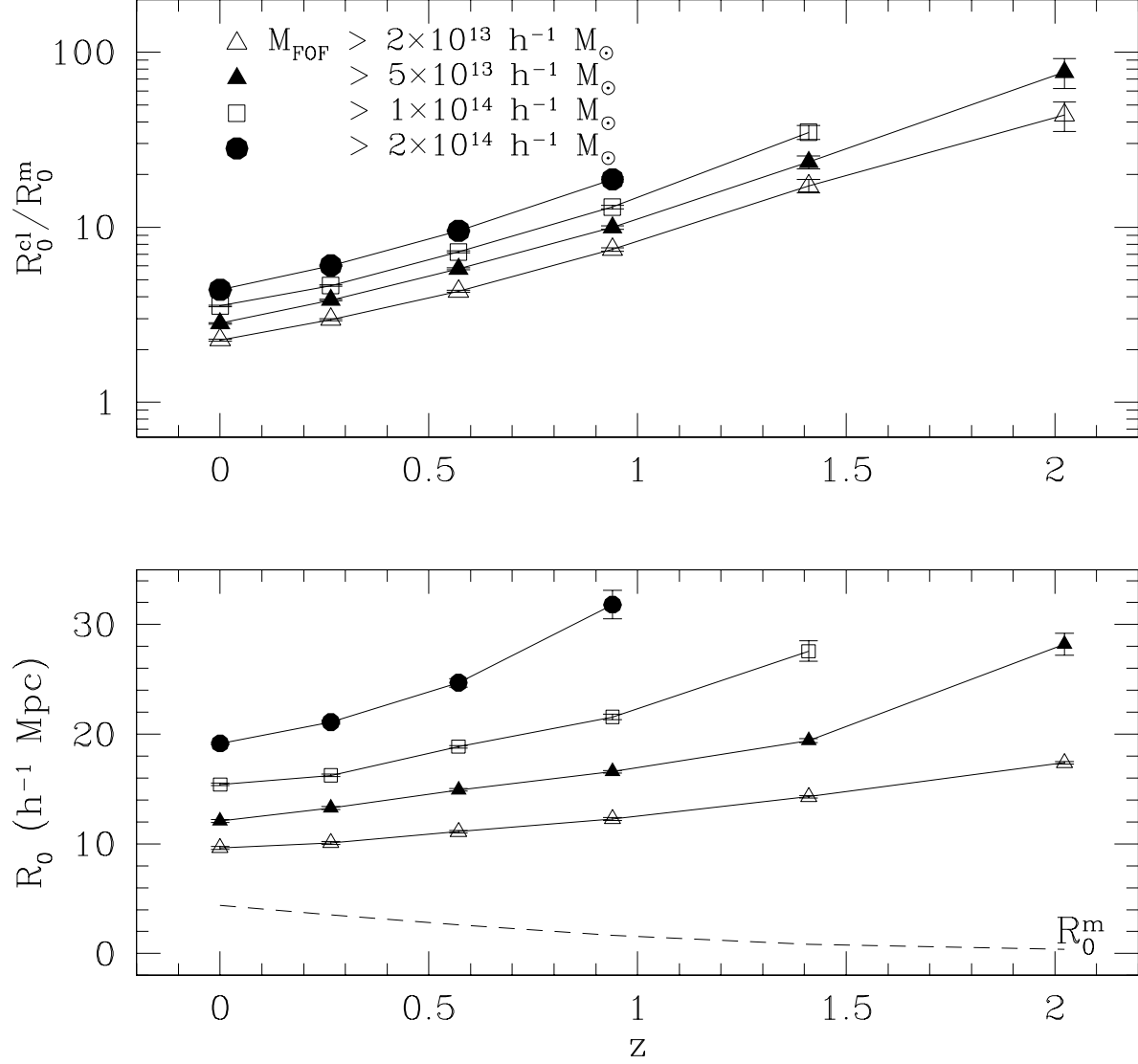


Fig. 6.— The ratio of the correlation scale of clusters (R_0^{cl}) to that of the underlying mass distribution (R_0^m) as a function of redshift for different mass thresholds. Also shown are the evolution of R_0^m (dashed line) and R_0^{cl} , separately.

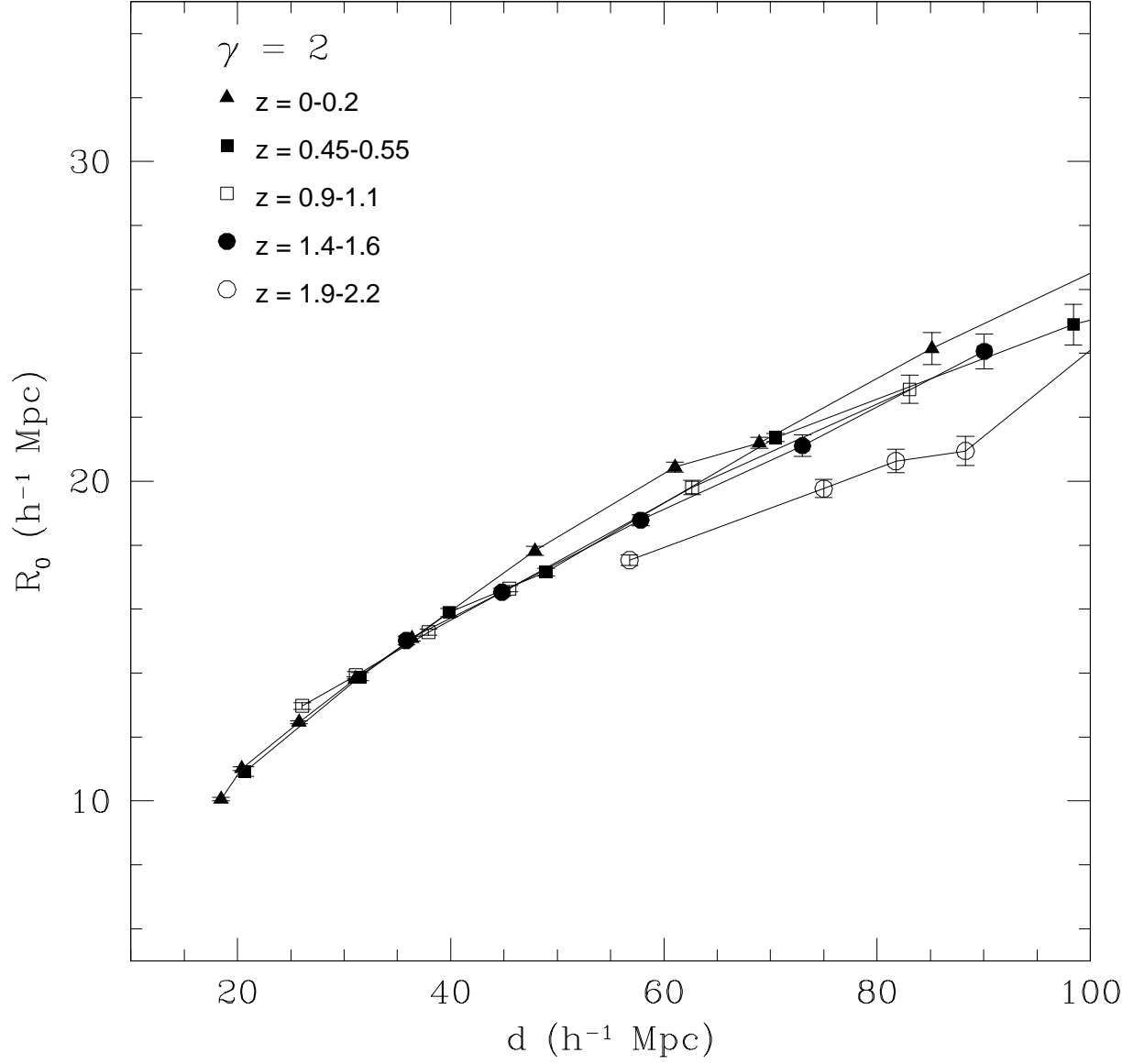


Fig. 7.— The evolution of the richness-dependent cluster correlation function : the $R_0 - d$ relation (comoving coordinates) for different redshifts using a fixed correlation slope $\gamma = 2$.

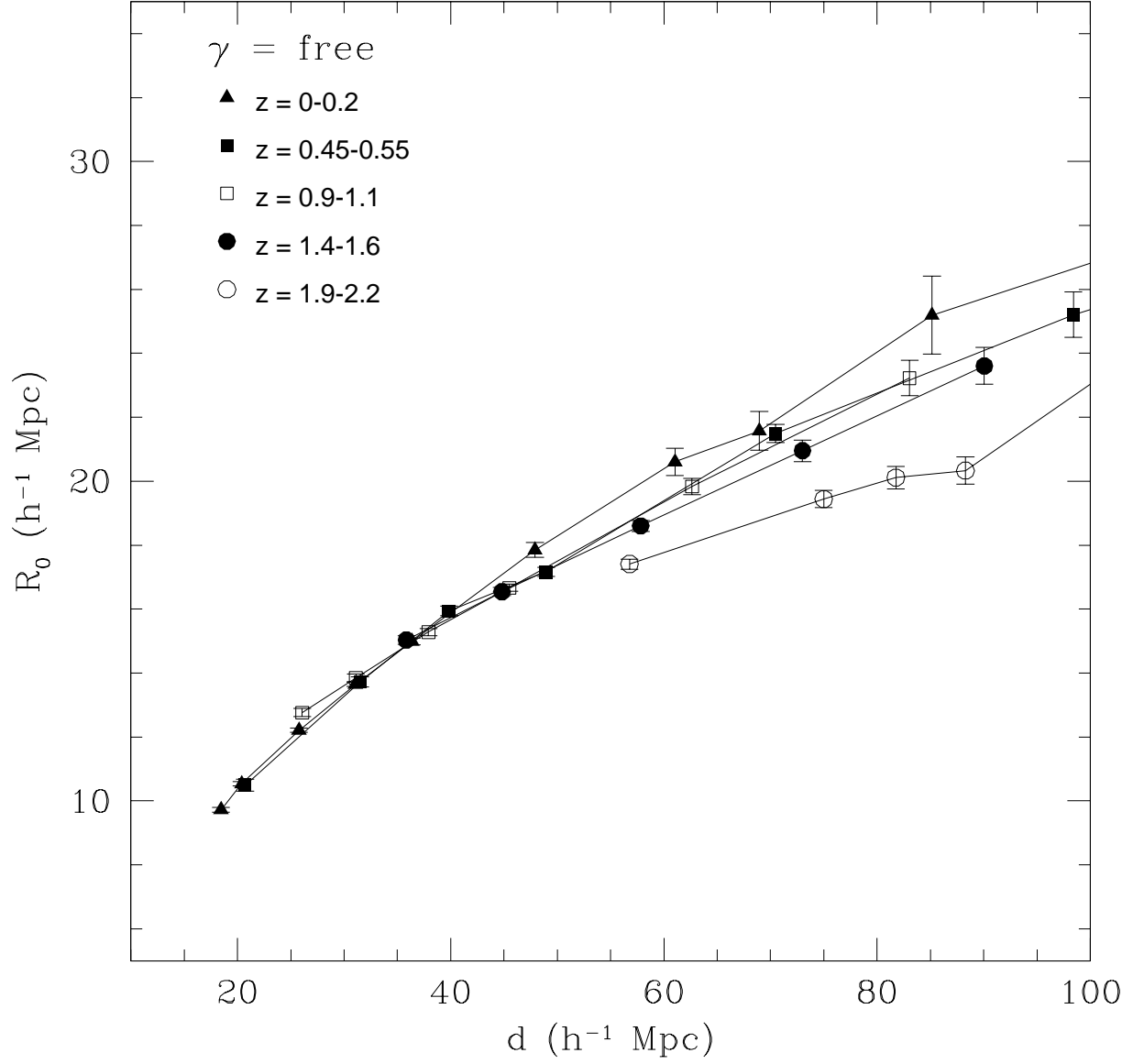


Fig. 8.— The R_0 - d relation (comoving coordinates) for different redshifts using a free-fitting correlation slope (γ).

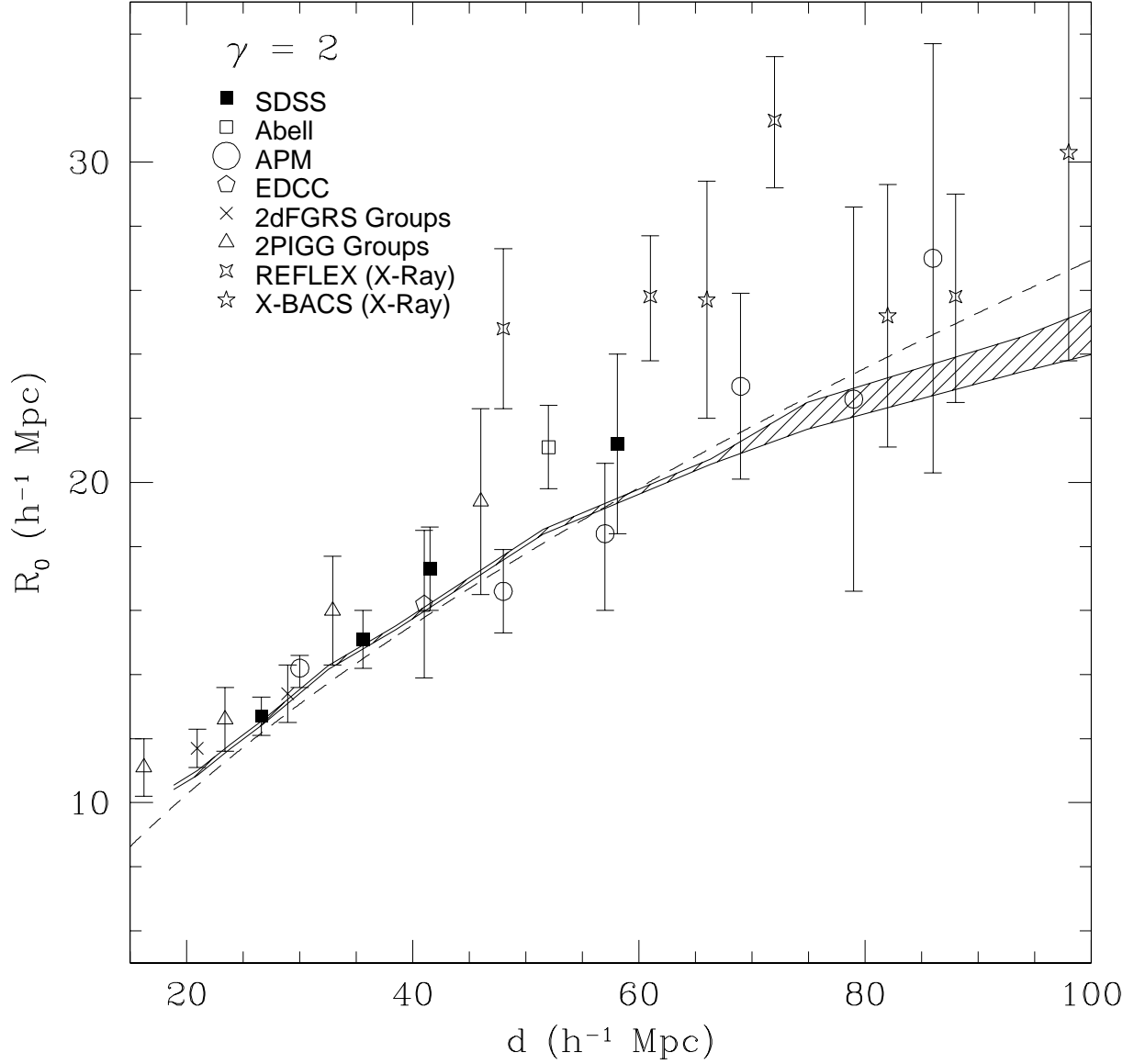


Fig. 9.— A comparison between the Λ CDM model $R_0 - d$ relation (shaded band; $z=0-0.3$) and observational results for a fixed correlation slope $\gamma = 2$ (data compiled by Bahcall *et al.* 2003c, with the addition of the 2PIGG groups from Padilla *et al.* 2004). The dashed line is a best fit power law approximation: $R_0 = 1.7d^{0.6}h^{-1}$ Mpc.